Appl. Phys. A 77, 855–858 (2003)
DOI: 10.1007/s00339-002-1440-6

Applied Physics A
Materials Science & Processing

J.P. ZOU✉
Y.F. MEI
J.K. SHEN
J.H. WU
X.L. WU
X.M. BAO

Si-based nanoscale SiO_2 islands and light-emitting source array

National Laboratory of Solid State Microstructures and Department of Physics, Nanjing University, Nanjing 210093, P.R. China

Received: 8 February 2002/Accepted: 2 April 2002
Published online: 27 June 2003 • © Springer-Verlag 2003

ABSTRACT A SiO_2 nanoscale island array was fabricated on a Si substrate by using anodic porous alumina as a mask. Transmission electron microscopy observation and the atomic force microscopy pattern show that the arrangement of SiO_2 islands has a quasi-hexagonal symmetry. Ge ions with a dose of $1 \times 10^{17}\ cm^{-2}$ were subsequently implanted into the SiO_2 island array to form Ge-related light-emitting centers. The photoluminescence (PL) spectra of as-implanted and annealed samples show three PL bands at 370, 400 and 415 nm. Their intensities reach maximums in the sample with an annealing temperature of 700 °C. Spectral analysis suggests that the 370 and 415 nm PL bands arise from $\equiv$Ge$-$Ge$\equiv$ and $\equiv$Ge$-$Si defect centers, while the 400 nm PL is related to GeO color centers in the SiO_2 islands. The existence of these PL bands indicates the formation of a Si-based nanoscale light source array.

PACS 78.55.Mb; 42.72.Bj; 68.65.+g

Since a Si-based light source plays an important role in Si-based optoelectronic integration, much research has focused on Si-based light-emitting materials in recent years. However, in most nanostructured materials with light emission, the distribution of nanocrystallites is spatially disordered, and thus their light emissions should be a kind of microscale light source, not a nanoscale one. Recently, many methods such as electron beam lithography [1] and ion beam lithography [2] have been employed to fabricate the distribution-ordered nanostructures of crystallites. These methods have many advantages, but they require huge and expensive fabrication systems. Instead of these methods, anodic alumina, as a natural lithography method, is a relatively simple and inexpensive technique for fabricating the ordered nanostructures by using self-organization [3]. Anodic alumina has attracted considerable research interest because of its ordered honeycomb structure. Some ordered metal and semiconductor nanostructures have been achieved using anodic alumina as a mask [4–6]. Thus, anodic alumina is useful as a mask for fabricating ideal Si-based nanostructures.

In this paper, anodic alumina is directly formed on a Si substrate as a mask for fabricating various nanostructures. The formed anodic alumina membrane contacts with silicon substrates and has a packed array of columnar hexagonal cells with central, cylindrical, uniformly sized holes, which is similar to the conventional anodic alumina membranes. Such structural characteristics are beneficial to the formation of an ordered nanostructure. By using this kind of anodic alumina mask, we achieved a Si-based SiO_2 nanoscale island array, and further obtain a kind of Si-based nanoscale light source through Ge^+-implantation into the SiO_2 islands. Photoluminescence (PL) measurements of as-implanted and the annealed samples show three luminescent bands peaking at 370, 400 and 415 nm. The appearance of these PL bands indicates the formation of a Si-based nanoscale light source, which will have important applications in Si-based nano-optoelectronic integration.

A p-type, 0.5 Ω cm, ⟨100⟩-oriented silicon wafer was used as the substrate. After cleaning and removing the native oxidation layer, high-purity Al (99.99%) film with a thickness of 400 nm was deposited on the pretreated Si wafer by electron-beam evaporation. The vacuum chamber was maintained under a pressure of 2.5×10^{-6} Pa. The accelerating voltage of the electron beam is held essentially constant near 10 kV, and the electron gun current is 0.5 A. The deposited Al film has a good and clear surface, and thus can directly be used to carry out anodization. Subsequently, the Al/Si film was anodized in 15 wt. % dilute sulfuric acid electrolyte under a constant dc voltage of 20 V at 5 °C. Figure 1 shows a typical current density-etching time (i–t) curve in the process of anodization. Obviously, the curve in the A-B range is from the anodization of the Al film, similar to that of a conventional bulk Al [7], and that in the B-C range is from anodization of the Si substrate. The BC curve can be used to control the formation of both the anodic porous alumina and SiO_2 nanoscale island array. At point B, the anodization on the Al film has run to the Al/Si layer interface, and will start to thin the alumina barrier layer; in the meantime, it will oxidize the Si substrate to form a SiO_2 nanoscale island array, while the preformed anodic porous alumina serves as a mask. Cross-sectional and planar transmission electron microscope (TEM) observations (JEOL JEM-2000EX operated at 160 kV) were carried out

✉ Fax: +86-25/359-5535, E-mail: xmbao@nju.edu.cn

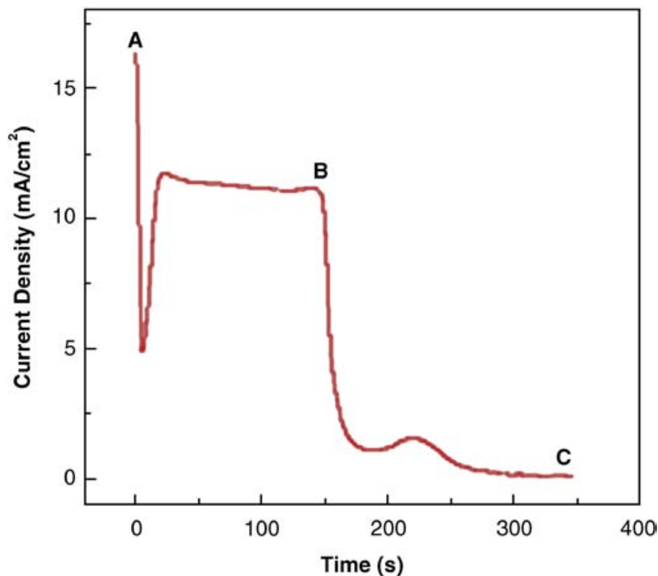

FIGURE 1 Current density vs. time transient curve for anodization of the Al/Si film at dc 20 V in 15 wt. % H_2SO_4 solution

on the Si-based anodic alumina mask. Figure 2 shows the corresponding cross-section TEM image. It can be seen that the parallel, straight and uniform alumina nanochannels with a mean diameter of about 14 nm have been fabricated on the Si substrate. At the bottom of each channel there is always an island. These islands construct an island layer. Fourier transform infrared spectrum shows that this island layer mainly consists of SiO_2. Since the SiO_2 only exists at the bottom of each channel, we may obtain a SiO_2 island array by removing the anodic alumina membrane.

After the sample was dipped in a 5 wt. % phosphoric acid solution at 30 °C for several hours, the anodic alumina membrane was automatically separated from the substrate. The microstructures of the separated anodic alumina mask and the substrate surface were characterized by means of TEM observation and an atomic force microscope (AFM) image, respectively. Figure 3a shows the planar TEM image of the anodic alumina mask. We can see from this image that the uniformly distributed and locally ordered nanoholes construct a nanohole array. The mean diameter of these nanoholes is

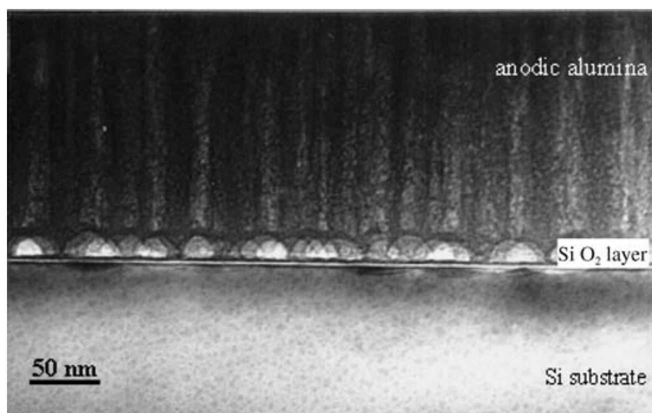

FIGURE 2 Cross-sectional TEM image of the Si-based anodic porous alumina

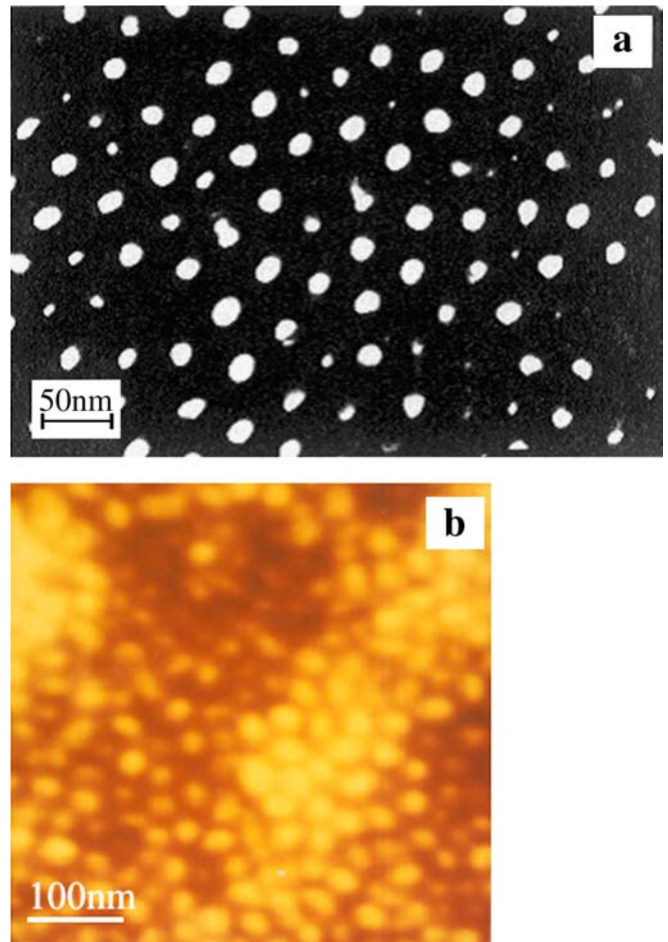

FIGURE 3 **a** Planar TEM image of anodic alumina mask; **b** AFM image of the SiO_2 nanoscale island array

about 15 nm, consistent with the value from Fig. 2. Figure 3b displays the AFM image of the SiO_2 nanoscale island array. The arrangement of the SiO_2 islands is in good agreement with that of the alumina nanoholes in Fig. 3a. Therefore, we believe that the regularity of the SiO_2 nanoscale islands is closely related to the anodic alumina mask. Because of the expansion effect in the process of oxidizing the Si, the mean diameter of the SiO_2 nanoscale islands is about 20 nm in Fig. 3b, which is larger than that of the corresponding nanoholes. In addition, as the anodization time increases, the diameter and thickness of the SiO_2 nanoscale islands increases. Since the thickness of the Al film is only 0.5 μm, the regularity of the anodic alumina nanoholes still needs improving to obtain a perfect SiO_2 island array.

After the SiO_2 nanoscale island array is formed, if a metal layer is deposited on the SiO_2 islands by the anodic alumina mask, a nanoscale MOS structure can be achieved. Furthermore, we have known that some Ge-related defects are efficient violet-emitting centers (e.g. 396 nm). If Ge ions are implanted into the SiO_2 islands to form these Ge-related defects, a nanoscale light source could be obtained.

As an example, here we explore the light-emitting property of this nanostructure. Along the vertical channels of the anodic alumina mask, Ge ions were implanted into the SiO_2 nanoscale island array at an energy of 200 keV and with

a dose of 1×10^{17} cm^{-2}, and then the mask was removed by a dipping treatment. Afterwards, the sample was annealed in N_2 ambient at 700, 800 and 1000 °C for 30 min. The PL measurements were performed at room temperature using a FluoroMax-2 photospectrometer. Figure 4 shows the PL spectra of the as-implanted and annealed SiO_2 nanoscale island arrays using an excitation wavelength of 248 nm (5 eV). The PL spectrum of the as-implanted sample exhibits three luminescent bands at 370, 400 and 415 nm. For the samples with a different annealing temperature (T_a), the positions of these PL peaks remains unchanged, but their intensities change with increasing T_a, reaching maximums in the sample with $T_a = 700$ °C. In the samples with T_a higher than 700 °C, the PL intensity dramatically decreases. It can be seen from Fig. 4 that the PL signal is weak, and the PL signal-to-noise ratio is relatively low in comparison to the PL from a Ge^+-implanted SiO_2 film grown by thermal oxidation. In a Ge^+-implanted SiO_2 nanoscale island array, light-emission bodies only exist in an individual nanoscale island, while light-emission bodies of Ge^+-implanted SiO_2 film pervade the entire microscale film region. From the point of view of statistics, when equi-area samples are excited under the same excitation condition, the luminescence intensities of the Ge^+-implanted SiO_2 nanoscale island array are obviously lower than those of the Ge^+-implanted SiO_2 film. So the PL signal-to-noise ratio of the former is very low. Since no PL was observed for the samples without Ge^+-implantation, we may infer that these PL bands originate from the SiO_2 nanoscale island array with Ge^+-implantation.

Ge^+-implantation into the SiO_2 nanoscale island array will lead to the formation of Ge-related defect centers.

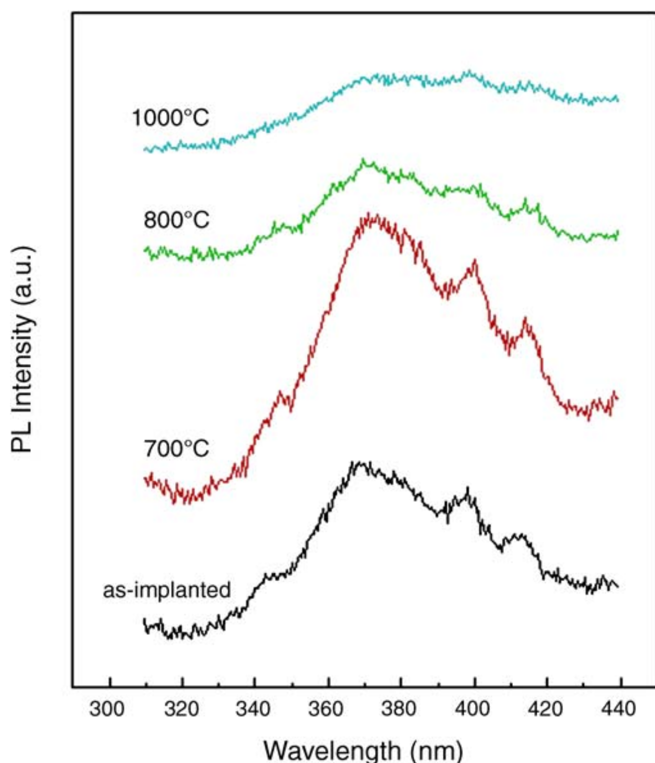

FIGURE 4 PL spectra of as-implanted and annealed SiO_2 nanoscale island array, taken under an excitation wavelength of 248 nm

Hosono et al. [8] have proposed that two types of oxygen-deficient (GODC) defect centers, Ge neutral oxygen vacancy center (GeNOV) and GeO color center, can be formed in Ge^+-implanted SiO_2 film. The neutral oxygen vacancy (NOV) is a result of Si–Si bond formation after removing one oxygen atom, which can be extended to Si–Ge and Ge–Ge bond formation in the case of Ge^+-implanted SiO_2. This results in three different types of oxygen vacancies, which are denoted as $\equiv$Si$-$Si$\equiv$, $\equiv$Ge$-$Si$\equiv$ and $\equiv$Ge$-$Ge$\equiv$ centers, respectively. We deduce that the 370 nm and 415 nm PL bands are closely related to the implantation-induced GeNOV centers, which may be explained as $T_1 \rightarrow S_0$ transition in the GeNOV centers. Since the SiO_2 becomes non-stoichiometric after Ge^+-implantation, the Si atom has the possibility of combining with another Si atom, which would form a Si–Si bond ($\equiv$Si$-$Si$\equiv$) in the SiO_2 islands. Further, we believe that one (or both) Si atoms in the $\equiv$Si$-$Si$\equiv$ center might be substituted by a Ge atom, which forms a $\equiv$Ge$-$Si$\equiv$ (or $\equiv$Ge$-$Ge$\equiv$) center. From the molecular spectroscopy [9], we know that when Ge ions substitute Si ions in the $\equiv$Si$-$Si$\equiv$ center, the $T_1 \rightarrow S_0$ transition energy will increase, and thus a blueshift of the PL peak from the ordered $\equiv$Ge$-$Si$\equiv$ or $\equiv$Ge$-$Ge$\equiv$ center can be expected compared with the 460 nm PL from the $\equiv$Si$-$Si$\equiv$ center. Therefore, we tentatively interpret the 370 nm and 415 nm PL bands as due to the $\equiv$Ge$-$Ge$\equiv$ and $\equiv$Ge$-$Si$\equiv$ defect centers in the Ge^+-implanted SiO_2 islands.

It is known that the 400 nm PL band from Ge-doped glasses is mostly related to optical transition in the GeO color center [10, 11]. The center is a Ge atom in the Ge^{2+} valence state bonded only to two oxygen atoms, instead of four as in the normal structure. As for the 400 nm (3.1 eV) PL band in Fig. 4, we may also attribute it to $T_1 \rightarrow S_0$ transition in the GeO center. When Ge ions are implanted into the SiO_2 islands, many Si–O bonds are destroyed and a great number of Ge, Si and O ions are produced. At low T_a, Ge$-$O (including GeO, Ge_2O_3 and GeO_2), Ge–Ge, Si–Si and Ge–Si bonds can be formed. Therefore, the PL peaks related to these bonds can appear with large intensities. At higher T_a, these bonds will also be annealed out, forming larger Ge clusters or Ge nanocrystals [12], and the Si oxide gradually becomes stoichiometric SiO_2. As a result, the observed PL band intensities decrease again.

In summary, we have directly fabricated an anodic alumina mask on a Si substrate. By controlling the anodization time, a SiO_2 nanoscale island array is formed at the bottom of the anodic alumina nanoholes. Ge ions were subsequently implanted into the SiO_2 nanoscale islands by the mask. The PL spectra of the as-implanted and annealed island array exhibit three PL bands at 370, 400 and 415 nm. We tentatively interpret the 370 and 415 nm PL bands as due to the $\equiv$Ge$-$Ge$\equiv$ and $\equiv$Ge$-$Si$\equiv$ defect center, while the 400 nm PL is related to GeO color centers in the SiO_2 islands. The existence of these PL bands indicates the formation of a Si-based nanoscale light source array.

ACKNOWLEDGEMENTS We thank Prof. R.Y. Chen of Beijing Normal University for ion implantation, Prof. M. Wang and Mr. X.B. Yin of Nanjing University for assistance on AFM measurements, and Mr.H. Chen

for PL measurements. This work was supported by Grants (Nos. 10225416, 10023001, and BK2002077) from the Natural Science Foundations of China and JiangSu province. Partial support was also from the Trans-Century Training Programme Foundation for the Talents by the State Education Commission and the Major State Basic Research Project No. G001CB3095 of China.

REFERENCES

1 W. Chen and H. Ahmed: Appl. Phys. Lett. **63**, 1116 (1993)
2 J.C. Wolfe, S.V. Pendharkar, P. Ruchhoeft, S. Sen, M.D. Morgan, W.E. Horne, R.C. Tiberio, J.N. Randall: J. Vac. Sci. Technol. B **14**, 3896 (1996)
3 H. Masuda, K. Fukuda: Science **268**, 1466 (1995)
4 P. Hoyer, N. Baba, H. Masuda: Appl. Phys. Lett. **66**, 2700 (1995)
5 D. Almawlawi, N. Coombs, M. Moskovits: J. Appl. Phys. **70**, 4421 (1991)
6 D. Almawlawi, C.Z. Liu, M. Moskovits: J. Mater. Res. **9**, 1014 (1994)
7 J.W. Diggle, T.C. Downie, C.W. Goulding: Chem. Rev. **69**, 365 (1969)
8 H. Hosono, Y. Abe, D.L. Kinser, R.A. Weeks, K. Muta, H. Kawazoe: Phys. Rev. B **46**, 11445 (1992)
9 S.P. McGlynn, T. Azumi, M. Kinoshita: *Molecular Spectroscopy of the Triplet State* (Prentice-Hall, Englewood Cliffs, NJ 1969)
10 M. Gallagher, U. Österberg: Appl. Phys. Lett. **63**, 2987 (1993)
11 T. Gao, X.M. Bao, F. Yan, S. Tong: Phys. Lett. A **232**, 321 (1997)
12 J.Y. Zhang, X.M. Bao, Y.H. Ye: Appl. Phys. Lett **73**, 1790 (1998)

Copyright © 2003 EBSCO Publishing